



# An evaluation of interferences in heat production from low enthalpy geothermal doublets systems



Cees J.L. Willems<sup>a, \*</sup>, Hamidreza M. Nick<sup>a, b</sup>, Gert Jan Weltje<sup>c</sup>, David F. Bruhn<sup>a, d</sup>

<sup>a</sup> Department of Geoscience and Engineering, Delft University of Technology, Delft, The Netherlands

<sup>b</sup> The Danish Hydrocarbon Research and Technology Centre, Technical University of Denmark, Copenhagen, Denmark

<sup>c</sup> Department of Earth and Environmental Sciences, University of Leuven, Belgium

<sup>d</sup> Helmholtz Centre Potsdam – GFZ German Research Centre for Geosciences, Germany

## ARTICLE INFO

### Article history:

Received 10 December 2016

Received in revised form

26 March 2017

Accepted 21 June 2017

Available online 22 June 2017

### Keywords:

Direct use geothermal energy

West Netherlands basin

Hot sedimentary aquifers

Common pool resource

## ABSTRACT

Required distance between doublet systems in low enthalpy geothermal heat exploitation is often not fully elucidated. The required distance aims to prevent negative interference influencing the utilisation efficiency of doublet systems. Currently production licence areas are often issued based on the expected extent of the reinjected cold water plume on the moment of thermal breakthrough. The production temperature, however, may not immediately drop to non-economic values after this moment. Consequently, heat production could continue increasing the extent of the cold water plume. Furthermore, the area influenced by pressure because of injection and production spreads beyond the cold water plume extent, influencing not only the productivity of adjacent doublet systems but also the shape of cold water plumes. This affects doublet life time, especially if adjacent doublets have different production rates. In this modelling based study a multi parameter analysis is carried out to derive dimensionless relations between basic doublet design parameters and required doublet distance. These parameters include the spacing between injector and producer of the same doublet, different production rates, aquifer thickness and minimal required production temperature. The results of this study can be used to minimize negative interference or optimise positive interference aiming at improving geothermal doublet deployment efficiency.

© 2017 The Authors. Published by Elsevier Ltd. This is an open access article under the CC BY license (<http://creativecommons.org/licenses/by/4.0/>).

## 1. Introduction

Low enthalpy Hot Sedimentary Aquifers (HSA) are often exploited by multiple individual geothermal operators with a single or a few doublet systems. Examples of this type of geothermal exploitation can be found in the West Netherlands Basin (WNB) and the Paris basin (e.g., [9,23]). Different geothermal operators may have different business cases with associated requirements for minimal production temperature, life time and heat production rate. In the WNB a geothermal production licence typically has an area which is equal to a rectangle with a size of  $L \times 2L$ , in which  $L$  is the injector to producer well spacing (e.g. [11,21]). This area should capture the extent of the cold water plume at the moment of

thermal breakthrough. After this moment, however, the production temperature may not necessarily drop immediately below non-economic values (e.g. Refs. [4,6,25]). In the WNB the production temperatures range from 70 °C to 90 °C, while the minimal required production temperature for economical HSA exploitation is 40 °C according to Pluymaekers et al. [16]. Obviously, continued production increases the extent of the cold water plume and thereby the area of influence of a doublet. Hence, the current licencing strategy may limit the recovery efficiency since the heat production could continue after the thermal breakthrough moment. In addition, doublet exploitation affects aquifer pressure distributions over much larger areas than the production licence (e.g. [11]). This could disturb injectivity and productivity of adjacent doublets. Moreover, it could influence the shape of the cold water plumes of adjacent doublets, thus, affecting their life time. This kind of interference becomes more pronounced when an adjacent doublet has a significantly higher production rate. In the Netherlands for example, current production rates vary from 100 m<sup>3</sup>/h to 300 m<sup>3</sup>/h (e.g. [5,12,16]) which may require a larger space between the

\* Corresponding author.

E-mail addresses: [c.j.l.willems@tudelft.nl](mailto:c.j.l.willems@tudelft.nl) (C.J.L. Willems), [hamid@dtu.dk](mailto:hamid@dtu.dk) (H.M. Nick), [gertjan.weltje@ees.kuleuven.be](mailto:gertjan.weltje@ees.kuleuven.be) (G.J. Weltje), [d.f.bruhn@tudelft.nl](mailto:d.f.bruhn@tudelft.nl) (D.F. Bruhn).

doublets. The current WNB licencing strategy may underestimate the required doublet distance which could eventually lead to an inefficient recovery and a negative interference.

The challenges of preventing interferences in a Common-Pool Resource are well known in exploitation of other types of geothermal resources than HSA. An example is shallow geothermal systems for Aquifer Thermal Energy Storage (ATES). However, these resources have different characteristics that influence interference. Unlike in HSA exploitation ATES systems operate periodically (and injection and production can be reversed). Therefore exploitation could be optimised in cycles based on experience from a previous cycle (e.g. [20]). In addition wells can easily be shut in and replaced by new ones on different locations to optimise exploitation due to significantly lower costs (e.g. [8]). A similarity between ATES and HSA exploitation is that doublet systems are often overdesigned and sub optimal use of the heat source is imminent [20,25]. In contrast, high enthalpy geothermal resources face a different challenge of over-exploitation. In this type of exploitation reinjection is not standard and hence pressure depletion plays a major role in interference (e.g. [10,22]). Compared to other types of geothermal resources, HSA are still a less established type of geothermal resource (e.g. [3]), albeit with a growing interest for heating purposes, not only in the Netherlands. To improve the potential of this type of resource it is of particular importance to reduce risks of negative interference and enhance potential recovery by optimising the layout and licencing of these type of systems.

The goal of this study is to better understand the required doublet distance as function of basic doublet design parameters. These parameters include injector to producer spacing, production flow rate, aquifer thickness and minimal required production temperature. The relation between these parameters and required doublet distance could be used to prevent negative interference, but also to optimise doublet deployment. This study is based on a case study of the West Netherlands Basin (WNB) where 15 doublets have been realised and 30 additional exploration licences were granted in the past 15 years. A modelling based approach is used in this study to explore the effect of doublet design parameters and doublet distance on interference in HSA exploitation. The design parameters ranges are derived from a WNB case study (e.g. [26]). Relations between doublet performance, doublet distance and the doublet parameters are derived from the multi-parameter analysis. These relations could be used to determine required doublet distance.

### 1.1. Interference and doublet configurations

In this study, two different doublet configurations are considered. If injectors and producers are aligned, this is referred to as the ‘tramline configuration’. In contrast, well functions can be alternated creating ‘checkboard’ pattern, which is referred to as “5-spot well layout” in the hydrocarbon industry [11]. showed that tramline configurations result in negative interferences in terms of life time and net energy production. Injectors increase the ambient aquifer pressure and therefore can reduce the injectivity of other neighbouring injectors. Producers act in the opposite way. As a result, the cold water plumes are narrower and cold water breakthrough occurs earlier. The opposite effect was recognized for checkboard configurations. In this configuration both life time and injectivity were enhanced. However, checkboard configurations could also induce cross flow between adjacent doublets. Fig. 1 illustrates both types of configurations, well spacing and doublet distance [11]. used only constant production rates in all doublets and the same well spacing and aquifer thickness throughout. However, production rate contrasts are likely to influence the interference. In

addition, the interference could be dependent on aquifer thickness and well spacing as these factors influence the net aquifer volume and hence the life time. For this reason, we included different production rates from neighbouring well doublets as well as variations in aquifer thickness and well spacing in our analysis.

## 2. Method

A 2D finite element (FE) approach was used to conduct a series of simulations for HSA exploitation with two doublets in the same aquifer. In these simulations doublet distance and other basic doublet design parameters were varied. These parameters included well spacing, production rates and Aquifer thickness. Here, the distance between wells in the same doublet was referred to as well spacing; the distance between wells of two adjacent doublets was referred to as doublet distance. The multi parameter analysis was carried out for both the checkboard and tramline configurations (Fig. 1). Based on these simulations the impact of the different parameters on doublet performance was evaluated in terms of life time, net energy production and NPV (add definitions of these terms as well). The doublet performance of the two doublets in tramline and the checkboard configurations was compared to production simulations with a single doublet with the same well spacing, aquifer thickness and production rate. Interference is expressed as deviation from the performance of a single doublet as a result of the proximity of another doublet.

### 2.1. Aquifer non-isothermal flow modelling

A  $9 \times 9$  km 2D, horizontal, homogeneous aquifer model, referred to as the interference model, is used for the production simulations in the interference study. The aquifer properties were derived from Nieuwerkerk Formation subsurface data (e.g. Refs. [4,21,26]). These properties are listed in Table 1. The aquifer properties are isotropic and only the rock matrix flow is taken into account assuming no presence of fractures.

The numerical modelling procedure follows the approach utilised by Refs. [18,19]. The energy balance was solved for a rigid medium fully saturated with water, in which thermal equilibrium was assumed between the fluid and solid phases:  $\rho C \frac{\partial}{\partial t} T + \rho_w C_w \nabla \cdot (\mathbf{q} T) - \nabla \cdot (\lambda \nabla T) = 0$ . In this balance,  $t$  [s] is time,  $T$  [K] is the temperature,  $\rho$  is the mass density [kg/m<sup>3</sup>],  $C_w$  [J/(kgK)] is the specific heat capacity,  $\lambda$  [W/(mK)] is the thermal conductivity tensor, and  $\mathbf{q}$  [m/s] is the Darcy velocity vector. The thermal conductivity is equal to  $\lambda_{eq} \mathbf{I} + \lambda_{dis}$ , and the volumetric heat capacity is described in terms of a local volume average. Where  $\lambda_{dis}$  is the thermal dispersion tensor and  $\mathbf{I}$  the identity matrix. The equivalent heat conductivity, density and the volumetric heat capacity are assumed to be independent of temperature for simplicity and described by  $\lambda_{eq} = (1-\phi)\lambda_s + \phi\lambda_w$  and  $\rho C = (1-\phi)\rho_s C_s + \phi\rho_w C_w$  in which  $\phi$  is the porosity. The thermal conductivity tensor is calculated through  $\lambda = (\lambda_{eq} + (\alpha_T)\mathbf{q})\mathbf{I} + \rho_f C_f (\alpha_L - \alpha_T) \mathbf{q}\mathbf{q}/|\mathbf{q}|$ . Where  $|\mathbf{q}|$  is the magnitude of the Darcy velocity vector and,  $\alpha_L$  and  $\alpha_T$  are the thermal dispersion coefficients in the longitudinal and transversal direction, respectively. This Darcy flow velocity vector can be determined by:  $\mathbf{q} = (k\nabla P)/\mu$ , where  $k$  [m<sup>2</sup>] the intrinsic permeability,  $\mu$  the temperature and salinity dependent viscosity like in Ref. [4], and  $P$  [Pa] the pressure. Temperature dependence of viscosity has a significant impact on cold water plume development and the approach used by Refs. [18,19] is applied to take this into account. The pressure field is obtained through solving the continuity equation:  $\phi(\partial\rho_w)/\partial t + \nabla \cdot (\rho_w \mathbf{q}) = \rho_w S$ , where  $S$  [1/s] is external sinks and sources. The suffix  $w$  refers to the pore fluid and  $s$  to the solid rock matrix. The values of all constant parameters are listed in Table 1. Triangular elements are used for the spatial discretisation

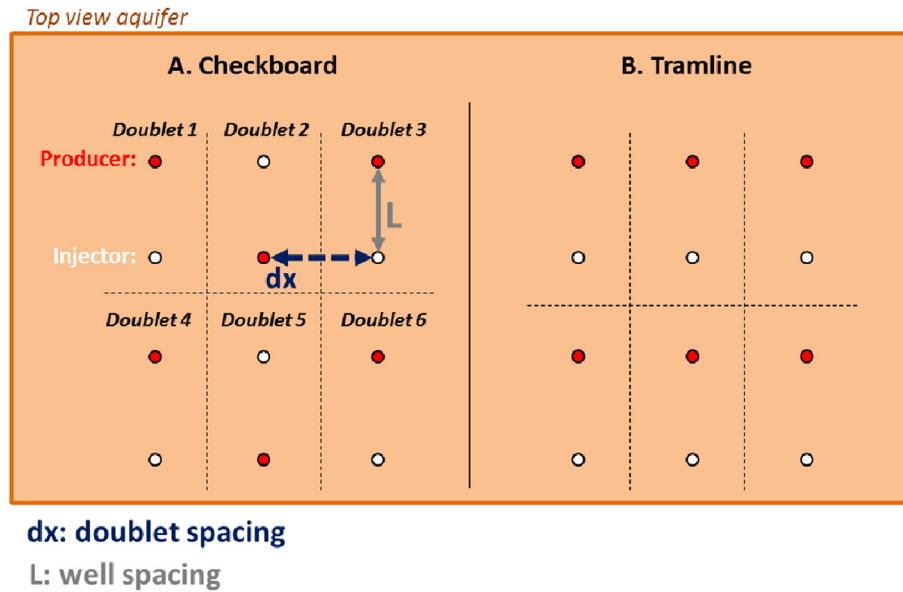


**Fig. 1.** Comparison of (A) checkboard configuration in which adjacent wells have opposite functions and (B) tramline configuration where the nearest well of an adjacent doublet has a similar function.

**Table 1**  
Aquifer and fluid properties used in the numerical simulations.

Parameter	Description	Interference model	Model 1	Model 2	Unit
$k_a$	Permeability of the sandstone	1000	1000	1000	mD
$\phi_a$	Porosity of the sandstone	0.28	0.15	0.10	–
$\lambda_a$	Conductivity of the sand bodies	2.7	2.7	2.7	W/m/K
$C_a$	Specific heat capacity of sandstone	730	730	730	J/kg/K
$\rho_a$	Density of sandstone	2650	2650	2650	kg/m <sup>3</sup>
$k_{shale}$	Permeability of the shale over- and underburden	–	–	0.01	mD
$\phi_{shale}$	Porosity of the shale over- and underburden	–	–	0.05	–
$\lambda_{shale}$	Conductivity of shale over- and underburden	–	–	2.0	W/m/K
$C_{shale}$	Specific heat capacity of shale over- and underburden	–	–	950	J/kg/K
$\rho_{shale}$	Density of shale over- and underburden	–	–	2600	kg/m <sup>3</sup>
$C_w$	Specific heat capacity of the brine	4200	4200	4200	J/kg/K
$\rho_w$	Density of brine	1050	1050	1050	kg/m <sup>3</sup>
$T_{res}$	Initial aquifer temperature	75	75	75	°C
$T_{inj}$	Reinjection water temperature	35	30	30	°C
$\alpha_L$	Longitudinal dispersion coefficient	10	0	0	m
$\alpha_T$	Transversal dispersion coefficient	1	0	0	m

that range in size from 0.2 near the wellbore to 150 m far away from the doublets. The production simulations yield a production temperature development over time and the required injection and production pressure for the associated production rate and set of parameters. The difference between these pressures ( $\Delta P$ ) was used to estimate pump energy losses:  $E_{pump} = \int_0^{LT} (Q \Delta P) / \epsilon dt$  (e.g. [27]), where  $Q$  is the production rate,  $LT$  the life time, and  $\epsilon$  the pump efficiency of 60%. The produced energy ( $E_{prod}$ ) was estimated by:  $E_{prod} = \int_0^{LT} Q \rho_w C_w \Delta T dt$  (e.g. [27]) in which  $\Delta T$  is the difference between injection temperature (35 °C) and production temperature. The net energy production was determined by the sum of the produced energy and the pump energy losses.

## 2.2. Model validation

A 2D model (Model 1) is used to validate the FE model result against an analytical solution [15]. In this model cold water (30 °C) is injected in a rectangular reservoir 10 m  $\times$  2000 m from one of the

short edge and warm water is produced from the other short edge. On the other long boundaries insulated and no flow boundary conditions are applied. The injection Darcy velocity is  $1 \times 10^{-6}$  m/s. Other model parameters are listed in Table 1. The initial aquifer temperature of this 2D model was 75 °C and reinjection water was 30 °C. Fig. 2-A illustrates a good fit between the model results and the 1D analytical solution of [15].

In order to evaluate the impact of the 2D model simplifications made in this study on the results, a more realistic 3D numerical model with an injection well and a producer well is designed (Model 2). The 3D model consists of three horizontal layers: overburden, permeable geothermal aquifer and underburden formation. Each layer has a thickness of 50 m. The model dimension is 1000 m  $\times$  500 m  $\times$  150 m. Cold water (30 °C) is injected with a discharge of 100 [m<sup>3</sup>/h]. Production simulations with and without temperature dependence of fluid viscosity and density are conducted. Simulation results of all 3D scenarios were compared to production simulations with a 2D model utilised in this study for the interference analysis (Fig. 2-B). In the 2D model the effects of

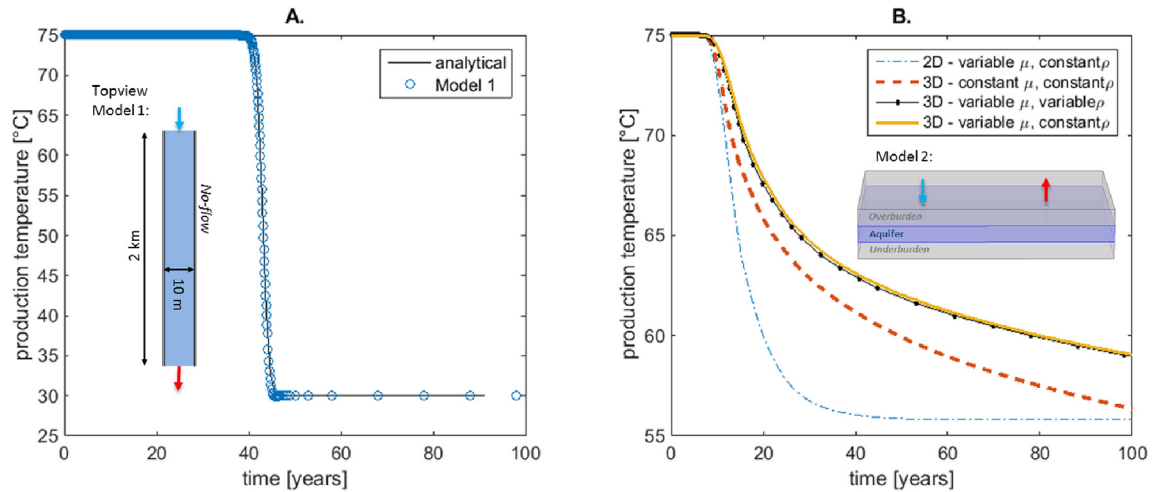


Fig. 2. (A) Temperature breakthrough calculated utilising the FE numerical model and the analytical solution. (B) Temperature breakthrough calculated for the 2D and 3D models.

density driven flow (e.g. Ref. [13]) and the over- and under-burden (e.g. Ref. [19]) on flow and heat transport are ignored. It can be seen in Fig. 2-B that the difference between the results of the models with and without density driven flow is very small. The effect of variable viscosity (i.e. temperature-dependent viscosity) is noticeable and therefore the fluid viscosity in the 2D interference model is temperature-dependent. The breakthrough results show a clear impact of under- and overburden on heat transfer. The cold water breakthrough time is one year shorter for the 2D model. Not surprisingly, the rate in which produced water temperature decreases is much higher for the 2D model compared to that of the 3D model. This positive effect on the produced heat is mainly due to the impact of the under- and overburden layers on heating the geothermal aquifer. In this study we are mainly evaluating the deviation of life time, net energy production and NPV calculated for two doublets with those of a single doublet. This implies that the effect of neglecting under- and overburden layers on the interference analysis is minimised. For the sake of reducing the computational time, the under- and overburden layers are not considered in the 2D interference model.

### 2.3. Net present value model

A NPV model developed by Ref. [24] was utilised in this study.

**Table 2**  
Economic parameters for the NPV realisation based on [24].

Economic parameters	Value	Unit
Heat price	€ 6.00	€/GJ
Electricity price for operations	€ 22.22	€/GJ
discount rate	7	%
CAPEX		
Well costs	€ 1.5	M€/km
Pump	€ 0.50	M€
Heat Exchanger	€ 0.10	M€
Separator	€ 0.10	M€
Contingency costs (10%)	€ 0.89	M€
SEI (drilling insurance)	€ 0.69	M€
OPEX	5	% of CAPEX/year
Tax	25.5	% of taxable income
Depreciation period	10	years
<b>Feed-in tariff (SDE+)</b>		
Base energy price (2015)	€ 0.052	€/kWh
contribution SDE+	€ 9.17	€/GJ

Input for the NPV calculations were the net energy production in Watt and the economic parameters listed in Table 2. In our study, additional separator costs were included, because in many WNB doublets natural gas co-production occurs. The NPV is the depreciated, discounted, net-cumulative income after 15 years. This period was chosen, because it is the maximum duration of the Dutch feed-in tariff scheme (SDE+) for geothermal energy [23]. Pump work-over costs of 0.25 M€ were taken into account every five years, which is equal to half of the estimated pump costs. A down-time of 40% was assumed for maintenance throughout the year.

### 2.4. Multi parameter analysis

The parameter value ranges were derived from WNB subsurface data and production data from currently active geothermal well doublets in the WNB [11,21,23,25] and are listed in Table 3. In the production simulations, different aquifer thicknesses of 25, 50 and 75 m were used. Well spacing is equal in both doublets; four different well spacing distances were used: 600, 800, 1000 and 1500 m. The distance between the two doublets ( $dx$ ) was varied from 4000 m to the well spacing ( $L$ ) minus 100 m in approximately 13 steps. Production rates in the simulations range from 50 m<sup>3</sup>/h to 300 m<sup>3</sup>/h in both doublets. Finally, the multi parameter analysis was carried out for both doublet configurations: checkboard and tramline (Fig. 3). In total some 10,000 simulations were conducted to analyse interference. In addition simulations were carried out with a single doublet with the same parameter value ranges for calibration of doublet performance.

### 2.5. Interference

The doublet performance for each set of parameters was

**Table 3**  
Parameter value ranges considered in the multi parameter analysis.

Parameter	Description	Value	Unit
H	Aquifer thickness	25, 50, 75	m
L	Doublet well spacing	600, 800, 1000, 1500	m
$dx$	Doublet distance	L-100 to 4000	m
$Q_1$	Flow rate doublet 1	50, 100, 150, 200, 250	m <sup>3</sup> /h
$Q_2$	Flow rate doublet 2	50, 100, 150, 200, 250, 300	m <sup>3</sup> /h

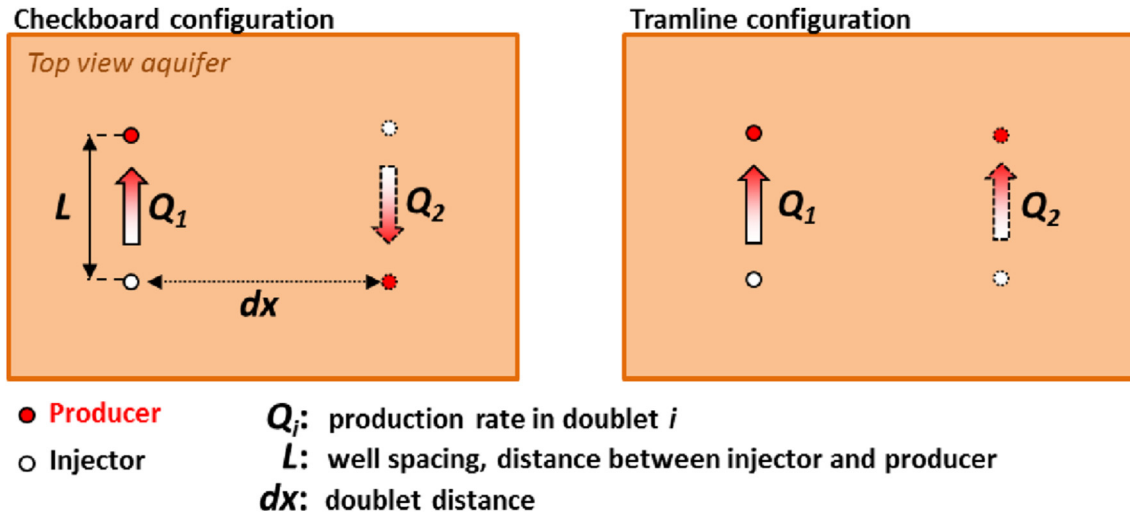


Fig. 3. Doublet configurations in the production simulations. The arrows indicate the main flow direction of the reinjected cold water towards the production well.

analysed in terms of (A) life time, (B) net energy production, and (C) Net Present Value (NPV). The life time of a doublet is reached when the production temperature decreased to a minimal allowed temperature ( $T_{\min}$ ). Three life time scenarios are compared (I)  $T_{\min} = 72.5$  °C, (II)  $T_{\min} = 70$  °C and (III)  $T_{\min} = 67.5$  °C. Interference is expressed as deviation from the performance of a single doublet. Life time interference ( $\Delta LT$ ) is defined as:

$$\Delta LT = (LT_{dx} - LT_{s,d})/LT_{s,d} \cdot 100\% \quad (1)$$

in which  $LT_{dx}$  is the life time of doublet 1 in a simulation with a certain doublet distance ( $dx$ ), well spacing ( $L$ ) and flow rate contrast.  $LT_{s,d}$  is the life time of a single doublet with the same parameter values. Interference in terms of net energy production ( $\Delta EP$ ) is defined in a similar way as:

$$\Delta EP = (EP_{dx} - EP_{s,d})/EP_{s,d} \cdot 100\% \quad (2)$$

In which  $EP_{dx}$  is the net-energy production of doublet 1 with a certain doublet distance ( $dx$ ) and  $EP_{s,d}$  is the net-energy production of a single doublet. Finally the effect of the interference on NPV of doublet 1 is defined as:

$$\Delta NPV = (NPV_{dx} - NPV_{s,d})/NPV_{s,d} \cdot 100\% \quad (3)$$

### 3. Results

#### 3.1. Area of influence of a single doublet

After thermal breakthrough, production temperature starts to decrease by approximately 2 °C per decade (Fig. 4-A). In this example the aquifer thickness is 75 m, the well spacing 1000 m and the production rate 150 m<sup>3</sup>/h. For instance, if the minimal production temperature is 70 °C, the life time of the doublet is 61 years. The cold water plume has a symmetrical tear-drop shape which is controlled by the streamline pattern. At the moment of cold water breakthrough the cold water plume lies within a rectangle with size 1000 m by 2000 m (Fig. 4-B1). However, if the life time is 61 years, the cold water plume extends beyond these boundaries (Fig. 4-B2). The fluid pressure distribution is constant over time and extends far beyond the rectangle boundaries. The pressure influence on the ambient aquifer pressure is limited. It changes the pressure by less than 1 bar at several hundred meters away from the wells.

#### 3.2. Area of influence, tramline configuration

The impact of doublet distance is quantified for doublets in tramline configurations. In Fig. 5 production temperature development of one of the two doublets is presented when the doublet distance ( $dx$ ) is 4000, 3000, and 1000 m. The production temperature development in these three scenarios is compared to that of a single doublet with the same well spacing, aquifer thickness and production rate. In this example the aquifer thickness is 75 m and the well spacing of both doublets is 1000 m. The doublets have equal production rates of 150 m<sup>3</sup>/h. When the doublet distance ( $dx$ ) is 1000 m the production temperature declines earlier and faster compared to the scenario with a doublet distance of 3000 m. For two systems with a doublet distance of 4000 m the production temperature development is almost equal to that of a single doublet.

These observations can be explained by the temperature- and pressure distribution development around the wells as well as the streamline patterns (Fig. 6). In tramline configurations, the proximity of the adjacent injector deforms the cold water plume (e.g., Fig. 6-A). The asymmetrical streamlines pattern in this figure confirms that flow velocity is higher in between the two doublets. As a result, the cold water plumes have a narrower tear-drop shape with a smaller doublet distance. In contrast, the cold water plume expands in a more symmetrical way when the doublet distance is 4000 m (Fig. 6-B). Nevertheless, the pressure distribution is still influenced as is reflected by the asymmetrical shape of the contour lines in Fig. 6-B. The production licence area is equal to a rectangle with sides  $dx+L$  and  $dx$ , in which  $dx$  is doublet distance and  $L$  is well spacing. Comparison of Fig. 6-A and B indicates that with larger doublets distance, a much larger part of the aquifer will be left unutilised.

#### 3.3. Area of influence: checkboard configurations

The impact of doublet distance is quantified for doublets in checkboard configurations. The results indicate that the thermal breakthrough time is delayed by several years when compared to a single doublet, for a model with the checkboard configuration with a doublet distance equal to the well spacing (Fig. 7). After thermal breakthrough however, temperature reduction is faster compared to that of a single doublet. No noticeable interference occurs if the doublet distance is 4000 m, as the production temperature

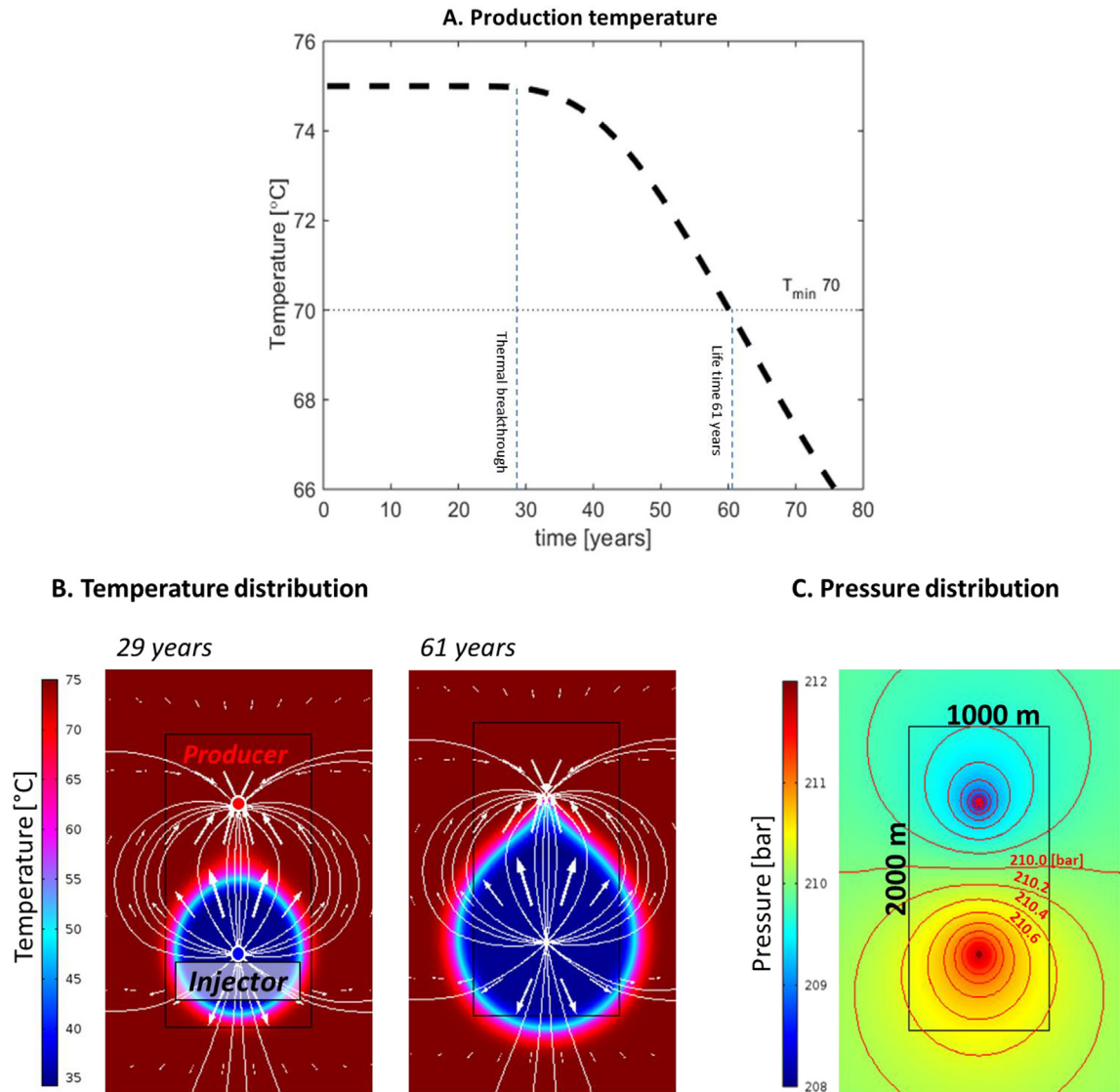


**Fig. 4.** (A) Development of production temperature of a single doublet. (B) Temperature distributions, streamlines and velocity vectors in the aquifer after 29 and 61 years. (C) Pressure distribution around the wells. Contour lines indicate a 0.2 bar transition. The black rectangle indicate a standard WNB production licence with the size of  $L \times 2L$ , in which  $L$  is the well spacing. The temperature and pressure distributions are sampled from the  $9 \times 9$  km aquifer model.

development is equal to that of a single doublet. When the doublet distance is 1500 m (i.e. 1.5 times the well spacing), the delay in thermal breakthrough is even larger. These results indicate that an optimum in life time interference could be found when doublet distance is larger than the well spacing and smaller than 4000 m.

In addition, the result in Fig. 7 indicate that the doublet distance affects the rate of production temperature reduction after the thermal breakthrough moment influencing the doublet life time. Therefore, the life time of a doublet in the checkboard configuration could be lower than that of a single doublet depending on the minimal required production temperature, despite the delay in thermal breakthrough time. For example, in case of a minimum production temperature of 70 °C, the life time of a single doublet is larger than the life time of a doublet in the checkboard configuration and a doublet distance of 1000 m.

Fig. 8 illustrates that checkboard configurations result in wider cold water plumes compared to tramline configurations (Fig. 6-B). Streamlines are less dense indicating that reinjected water flows less fast towards the producers. This prolongs the thermal

breakthrough time. For the case of the doublet distance equal to 1000 m, the cold water plumes cross the production licence boundaries after 30 years. With this doublet distance, the reinjected water flows to both adjacent production wells with the same rate. As a result of this cross flow between the doublets, the production temperature reduces faster after the thermal breakthrough moment. If the doublet distance is larger than the well spacing, e.g. 1500 m (Fig. 8-B), the cold water plumes do not cross the production licence boundaries before the thermal breakthrough moment.

#### 3.4. Interference as a function of doublet distance

Interference is evaluated in terms of life time, net energy production and NPV as functions of doublet distance (Fig. 9). Interference is expressed as deviation of doublet performance from that of a single doublet. If  $\Delta LT$ ,  $\Delta EP$  or  $\Delta NPV$  is 0, no interference occurs. Fig. 9-A to C relate to interference in tramline configurations, and Fig. 9-D to F relate to interference in checkboard configurations. The

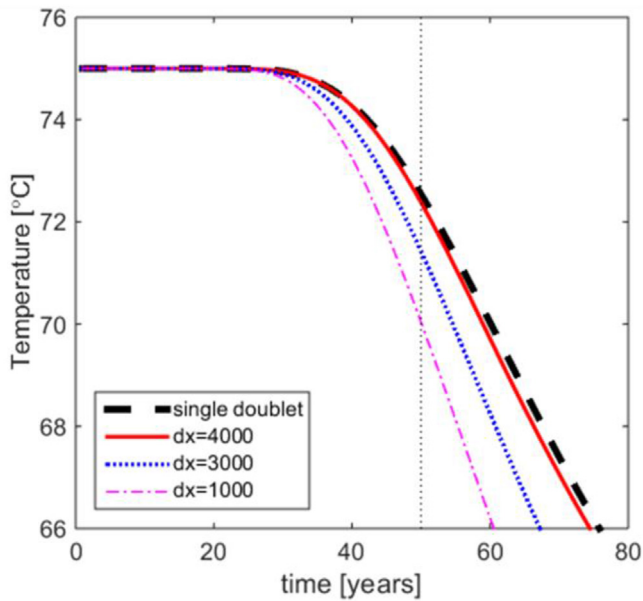


Fig. 5. A) Development of production temperature of one of the two doublets in the tramline configuration. The well spacing in both doublets is 1000 m and their production rate is  $150 \text{ m}^3/\text{h}$ .

results show that interference is always negative in tramline configurations unless the doublet distance is 4000 m or more, which is 4 times the well spacing in this example. Furthermore, Fig. 9

indicates that interference is most significant in terms of life time.  $\Delta EP$  and  $\Delta NPV$  in these results were smaller than 0.1% while  $\Delta LT$  varies more significantly from 0 to 30% depending on the doublet distance and doublet configuration. The minimal production temperature has a small effect of several percentages on the life time.  $\Delta LT$  is larger if  $T_{\min}$  is lower in the tramline configuration. In the checkboard configuration, an optimum in positive interference is recognized. This optimum shifts to higher doublet distance for lower  $T_{\min}$ .

### 3.5. Interference and production rate contrast - tramline

A difference in production rate between doublet 1 and 2, henceforth referred to as production rate contrasts, increases interference and the required doublet distance in tramline configurations. This is derived from Fig. 10-A to C. In this figure the relation of  $\Delta LT$  and doublet distance is presented for different production rate contrasts. A dimensionless production rate contrast ( $dQ$ ) is defined as:  $dQ = (Q_2 - Q_1)/(Q_2 + Q_1)$ . The interference is more significant in the doublet with the lower production rate. This can be seen in Fig. 10-B and C where  $\Delta LT$  is larger for doublet 1 which has a lower flow rate than doublet 2. Therefore the required doublet distance should be determined from the perspective of the doublet with the lowest production rate. In tramline configurations interference will always reduce life time unless very large doublet distance of approximately four times the well spacing or more is considered (Figs. 7 and 9). In Fig. 10-C two examples of determination of minimal doublet distance are shown when the production rates in doublet 1 and 2 are  $50 \text{ m}^3/\text{h}$  and  $200 \text{ m}^3/\text{h}$ , respectively. If

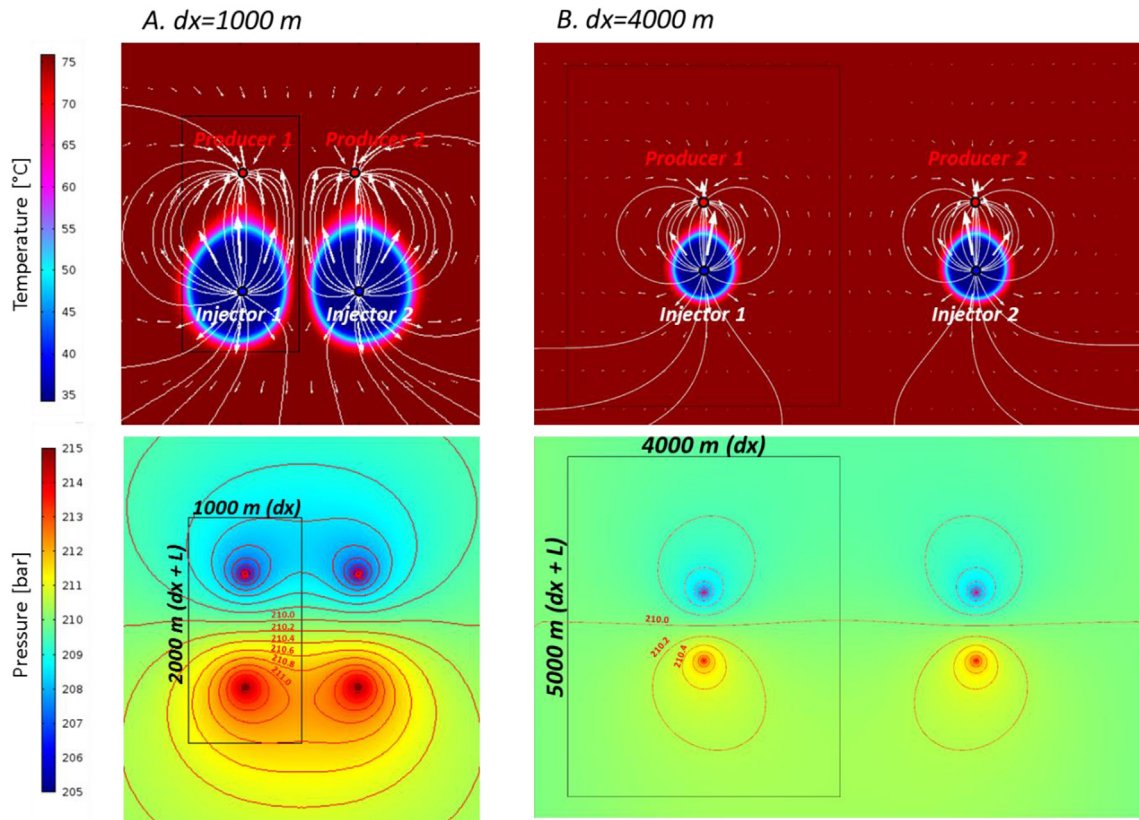
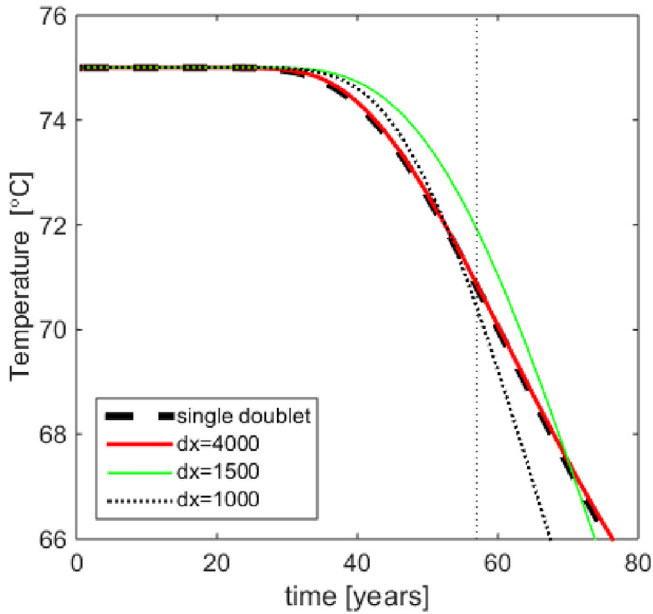


Fig. 6. Temperature and pressure distribution in the aquifer after 30 years for (A) doublet distance  $dx = 1000 \text{ m}$  and (B) doublet distance  $dx = 3000 \text{ m}$ . Streamlines and velocity vectors are illustrated in the temperature plots. Contour lines indicate a 0.2 bar transition in the pressure distribution plots. The black rectangle indicates the production licences in both scenarios A and B. The aquifer thickness is 75 m, the well spacing ( $L$ ) in both doublets is 1000 m and their production rate is  $150 \text{ m}^3/\text{h}$ . The temperature and pressure distributions are sampled from the  $9 \times 9 \text{ km}$  aquifer model.



**Fig. 7.** Production temperature development of one of the two doublets in the checkboard configuration. The aquifer thickness is 75 m, the well spacing in both doublets is 1000 m and their production rate is 150 m<sup>3</sup>/h.

the accepted life time reduction is 15% the minimal distance is approximately 1950 m. In case the accepted life time reduction is only 5%, the required doublet distance is 3600 m.

### 3.6. Minimal doublet distance - tramline

Following the example in Fig. 10-C, the minimal doublet distance for doublets in tramline configurations is determined for all well spacing, production rate contrasts, aquifer thickness scenarios and for  $\Delta T$  of  $-5\%$  and  $-15\%$ . Fig. 11 presents the resulting relations between the minimal doublet distance and dimensionless production rate contrast  $dQ$ . In this figure the minimal production temperature ( $T_{min}$ ) is 70 °C.  $dQ$  is defined as:  $dQ = (Q_2 - Q_1)/(Q_2 + Q_1)$ , in which  $Q_1$  and  $Q_2$  are the production rates of doublet 1 and 2, respectively. In Fig. 11-A the accepted  $\Delta T$  is 15% and in Fig. 11-B accepted  $\Delta T$  is 5%. It can be seen that  $dx_{min}$  increases for increasing production rate contrasts. Furthermore  $dx_{min}$  is larger for doublets with larger well spacing. In Fig. 11-C and D, the minimal distance is normalised by division of  $dx_{min}$  by the associated well spacing. The normalised relation between doublet distance and production rate contrast shows that  $dx_{min}/L$  is independent of the aquifer thickness. The minimal distance is significantly higher when the allowed negative interference is smaller, i.e. when  $\Delta T$  is 5% instead of 15% (Fig. 11-A and B). For example, when the allowed accepted  $\Delta T$  is 15% and two doublets in the tramline configuration have an equal production rate, the required doublet

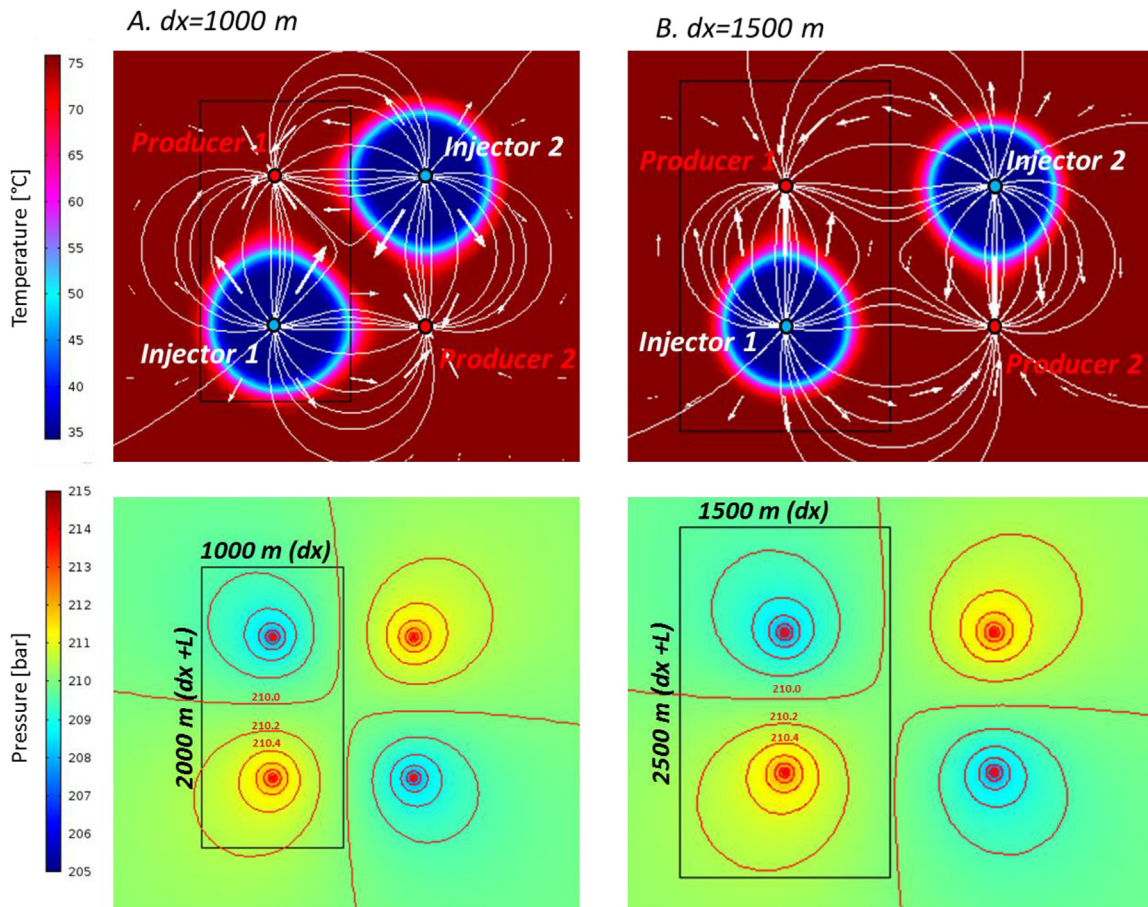


**Fig. 8.** Temperature and pressure distribution in the aquifer after 30 years for doublet distance ( $dx$ ) of (A) 1000 m and (B) 1500 m. Streamlines and velocity vectors are shown in the temperature plots. Contour lines indicate a 0.1 bar transition in the pressure distribution plots. The black rectangle demonstrates the production licences. The aquifer thickness is 75 m, the well spacing in both doublets is 1000 m and their production rate is 150 m<sup>3</sup>/h. The temperature and pressure distributions are sampled from the 9 × 9km aquifer model.



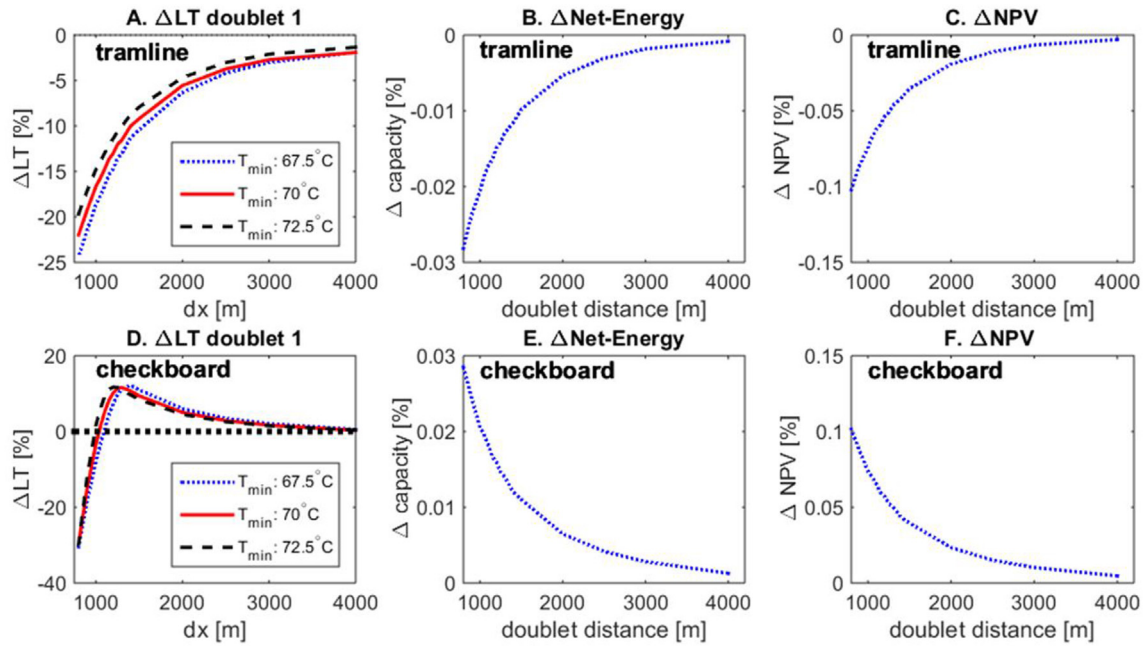


**Fig. 9.** Comparison of the performance of a single doublet to a doublet in the tramline configuration (A,B,C) and the checkboard configuration (D,E,F). In A and D the interference is expressed in terms of life time ( $\Delta LT$ ) for three different minimal production temperatures. In B and E interference is expressed in terms of net-energy production ( $\Delta EP$ ) and C and F show interference in terms of net present value ( $\Delta NPV$ ).

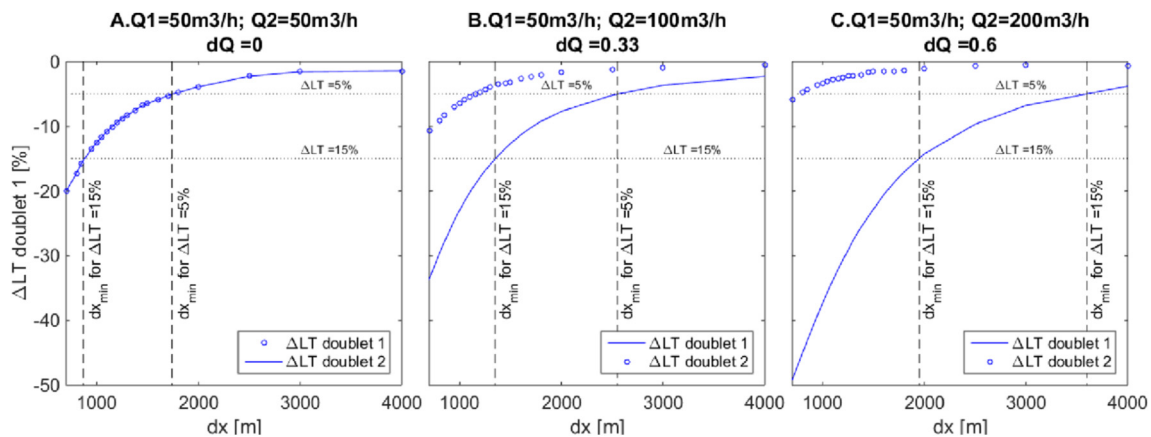


**Fig. 10.** Life time interference of doublet 1 and 2 in the tramline configuration, for different production rate contrasts as function of doublet distance. Minimal production temperature is  $70^\circ C$  in this example. In A the production rate is equal in both doublets. In B the production rate contrast is  $50 m^3/h$ , and in C the production rate contrast is  $150 m^3/h$ . In these examples, the aquifer height was 75 m and the well spacing 800 m.

distance is approximately 1.15 times the well spacing of the life time of both doublets is (Fig. 11-A). This increases to 2.1 when the allowed life time reduction is only 5% (Fig. 11-B). Note that maximum production rate contrast with a well spacing of 1500 m is only displayed for values of  $dQ$  up to 0.3. This is because the maximum and minimum production rates are  $300 m^3/h$  and  $150 m^3/h$ , respectively. For lower production rates below  $150 m^3/h$  that would result in larger contrasts, the life time of the doublet were longer, longer than 250 years, especially for  $T_{min}$  of  $67.5^\circ C$  and  $70^\circ C$ .

Subsequently the normalised relation of doublet distance and  $dQ$  is determined for three different minimal production temperature scenarios: (A)  $T_{min}$  is  $67.5^\circ C$ , (B)  $T_{min}$  is  $70^\circ C$  and (C)  $T_{min}$  is  $72.5^\circ C$ . The results in Fig. 12 show that if  $T_{min}$  is lower,  $dx_{min}/L$  increases. Required doublet distance is therefore dependent on

$T_{min}$ . This is a result of impact of doublet distance on the rate of the production temperature reduction as shown in Fig. 5. This figure shows that doublet distance influences the rate of production temperature reduction after thermal breakthrough. Because of this effect and because interference is calibrated on the performance of a single doublet in our study, a larger doublet distance is required to compensate when the minimal production temperature is lower.

### 3.7. Interference and production rate contrast - checkboard

Production rate contrasts influence optima in positive life time interference. This is derived from Fig. 13. In this figure the relation of  $\Delta LT$  and doublet distance is presented for doublets in checkboard configurations with different production rate contrasts ( $dQ$ ). The

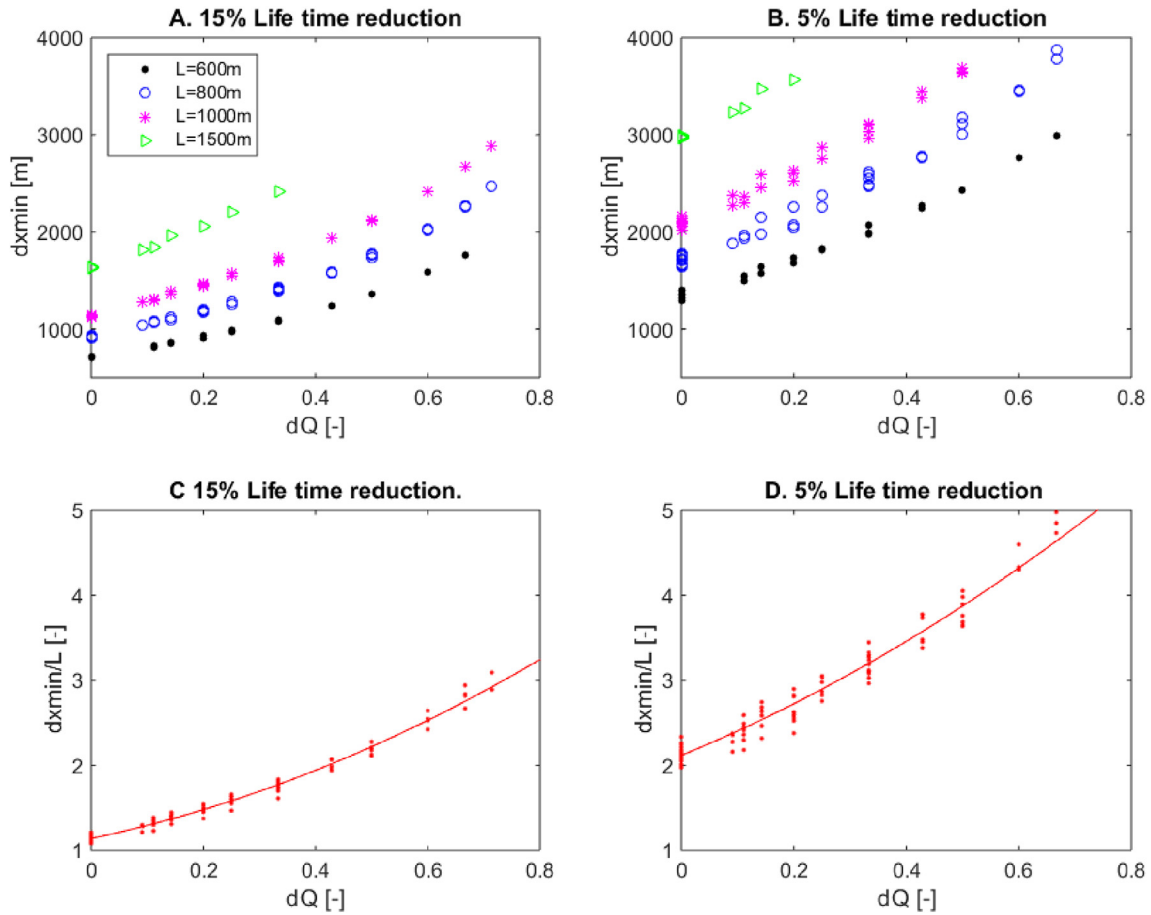


**Fig. 11.** (A) Relation of minimal doublet distance and production rate contrast ( $dQ$ ) for a 5% life time reduction in the tramline configuration. (B) Relation of minimal doublet distance and production rate contrast ( $dQ$ ) for a 15% life time reduction in the tramline configuration. (C) Normalised minimal doublet distance of A, (D) Normalised minimal doublet distance of B. For all figures the life time is determined for a minimal production temperature of 70 °C.

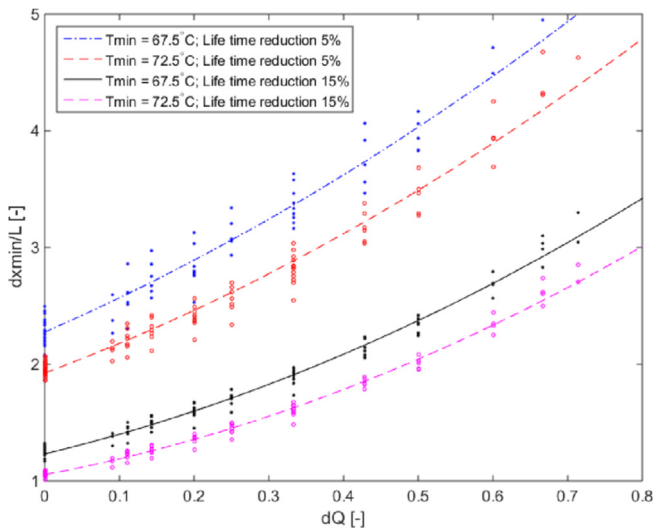


**Fig. 12.** Dimensionless relations between minimal doublet distance and flow rate contrast for different minimal production temperature and for a 5% and 15% life time reduction in the tramline configuration.

relations indicate that positive interference is relatively larger in the doublet with the lowest production rate. In addition, the optima of the doublet with the lower production flow rate shift to large  $dx$

values if the production rate contrast ( $dQ$ ) increases. Oppositely, the optima for the doublet with the higher production rate shifts to lower  $dx$  values for higher  $dQ$  values.

The production rate contrast could also result in negative life time interference in the doublet with the lowest production rate, despite the checkboard configuration. An example is presented in Fig. 13-B. In this example, doublet 1 produces at 50 m<sup>3</sup>/h and doublet 2 at 100 m<sup>3</sup>/h. If the doublet distance is 750 m, an optimum in  $\Delta LT$  of approximately 5% in doublet 2 is obtained while the  $\Delta LT$  in doublet 1 is –15%. Doublet distance should be carefully chosen if doublets are placed in checkboard configurations, especially with a production rate contrast.

The results in Fig. 13 illustrate that optimal doublet distance ( $dx_{opt}$ ) for doublets in checkboard configurations could be chosen from 3 different perspectives. A first option is to choose  $dx$  to maximise positive interference in the doublet with the lowest production rate. An example is presented in Fig. 13-C. For a doublet distance of 1600 m, the  $\Delta LT$  in doublet 1 is 30% while the  $\Delta LT$  in doublet 2 is 0%. In contrast, optimal doublet distance could aim to maximise positive life time interference in the doublet with the highest production rate. An example is presented in Fig. 13-B. For a doublet distance of 900 m, the  $\Delta LT$  in doublet 2 is 5% while the  $\Delta LT$  in doublet 1 is –15%. Finally optimal doublet distance could be chosen as a compromise where the  $\Delta LT$  curves for both doublets intersect. This option is shown in Fig. 13-C by the vertical blue line with a  $dx = 900$  m. In that case  $\Delta LT$  is approximately 2% in both doublets. In this study, optimal doublet is determined such that

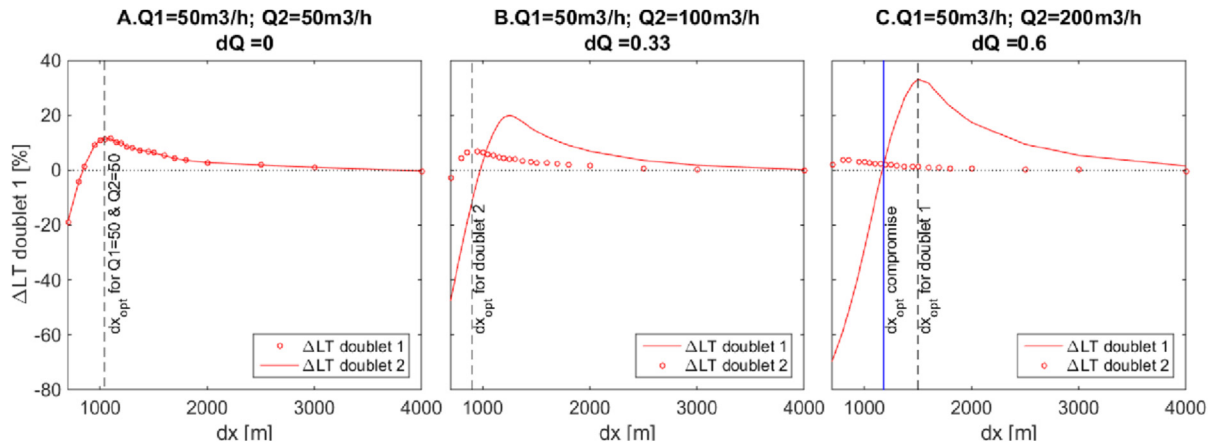


**Fig. 13.** Life time interference of doublet 1 and 2 in the checkboard configuration, for different production rate contrasts as function of doublet distance. Minimal production temperature is 70 °C in this example. In A the production rate is equal in both doublets. In B the production rate contrast is 50 m<sup>3</sup>/h, and in C the production rate contrast is 150 m<sup>3</sup>/h. In these examples, the aquifer thickness was 75 m and the well spacing 800 m.

interference is optimised for the doublet with the lowest production rate.

3.8. Optimal doublet distance - checkboard

The optimal doublet distance for doublets in checkboard configuration is determined for all well spacing, production rate, and aquifer thickness scenarios (Fig. 14-A). Note that this is optimised with respect to the doublet with the lowest production rate. Like in Fig. 11-C, the  $dx_{opt}$  values are normalised by division of  $dx_{opt}$  by the associated well spacing. The dimensionless relation of the ratio of  $dx_{opt}$  and well spacing to the dimensionless production rate contrast  $dQ$  is shown in Fig. 14-B. This figure indicates that the optimal doublet distance is increased when the  $T_{min}$  is lower. For example, for a minimal production temperature of 67.5 °C optimal doublet distance is approximately 1.3 times larger than the well spacing. For the higher minimal production temperature of 72.5 °C, this factor reduces slightly to 1.2. Therefore, optimisation of interference depends on the minimal allowed production temperature and the production rate contrast between both doublets and production rate contrast.

4. Discussion

4.1. Minimum production temperature

Our results indicate that an analysis of the minimal production temperature should be part of a doublet deployment strategy. Firstly, this is because this parameter is related to the life time and the maximum extent of the cold water plume. Our results underline the possibility for continued production after the thermal breakthrough moment as the production temperature only drops by a few degrees after several decades (Figs. 5 and 7). When thermal recharge from aquifer heterogeneities as well as over- and underburden were taken into account, the rate of production temperature reduction would be even lower [4,17,25]. In addition, lifetimes could be even longer if we took technical progress into account; lower production temperatures may well be sufficient in the future because heat insulation and heat exchanger efficiency are likely to improve in the next decades.

Secondly, the minimal production temperature is related to the required doublet distance as interference could affect the rate of temperature reduction after cold water breakthrough (e.g., Figs. 5

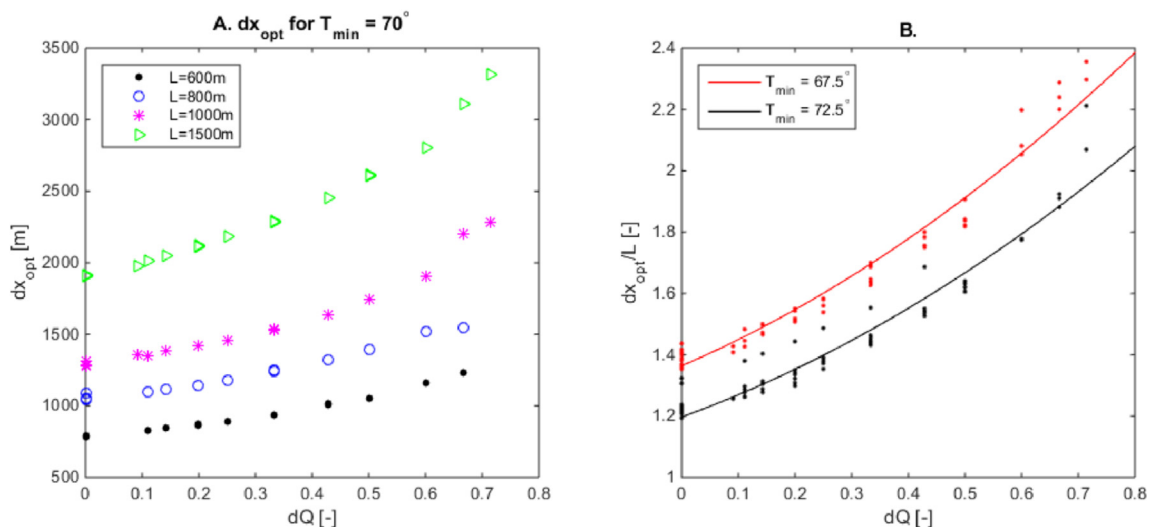


**Fig. 14.** (A) optimal doublet distance for the checkboard configuration as a function the dimensionless flow rate contrast  $dQ$ . (B) dimensionless ratio of  $dx_{opt}$  and well spacing ( $L$ ) as a function the dimensionless flow rate contrast.

and 7). In our evaluation, interference is calibrated to the performance of a single doublet with the same production rate, well spacing and aquifer thickness. Therefore the dimensionless relations between required doublet distance and production rate contrast that were derived are dependent on minimal production temperature to compensate for interference. Because of the current uncertainty in minimal production temperature for doublet systems, further study is required on this parameter to reduce future interference risks.

#### 4.2. Geological heterogeneity

In our study simplified homogeneous 2D models were used to derive the impact of doublet design parameters, such as well spacing, production rate and aquifer thickness, on interference. Our results showed that interference is mainly significant in terms of life time. This is because exploitation by nearby doublet systems changes the pressure distribution and hence the shape of the cold water plumes. The pressure change distribution is too small to affect injectivity and productivity significantly. Geological heterogeneities could affect our results by influencing pressure distribution. Such heterogeneities include facies architecture [4,26], small scale sedimentary features (e.g. [1]), faults and fractures [2,7,14] as well as aquifer thickness variation. Their impact on interference depends on the directional trend of the heterogeneities with respect to the location of the adjacent doublet. Different types of heterogeneities could either decrease or increase pressure communication between doublets. When the heterogeneities enhance pressure communication between adjacent doublets, larger doublet distance would be required compared to when flow baffles decrease pressure communication.

In addition, thermal recharge from over- and under-burden were neglected in our analysis. These factors will influence both the thermal breakthrough moment as well as the rate of production temperature decline (Fig. 2-B; [17–19]). The effect of thermal recharge on doublet life time is dependent on the aquifer thickness and the ratio of flow rate and conduction rate [17]. In this study, we defined interference as deviation in performance from that of a single doublet, which is less affected by the choice of the model. Employing a more realistic geological model will improve the predictive capability of the geothermal reservoir models [4,26].

#### 4.3. Tramline versus checkboard configurations

The definition of required doublet distance in this study is dependent on the doublet configuration. A differentiation is made between minimal required doublet distance and optimal doublet distance. Optimal doublet distance is defined as the doublet distance for which an optimum in positive interference is obtained. This is only possible when doublets are placed in the checkboard configuration. In contrast, minimal doublet distance aims to prevent negative interference. For doublets in checkboard configurations this minimal required distance aims to prevent cross flow of reinjected water between adjacent doublets. Cross flow could occur if the doublet distance is smaller than the injector-producer well spacing in checkboard configurations. In addition, it could be induced by production rate contrasts even if the doublet distance is larger than the injector-producer well spacing. When doublets are placed in tramline configurations, minimal doublet distance aims to minimize negative interference. In this configuration reinjected water is forced to flow faster towards the production well of the same doublet. Our results show that this effect cannot be avoided unless doublet distances of at least four times the well spacing are used. This factor could change if geological

uncertainties are taken into account. Nevertheless, these results imply that the required distance to avoid negative interference for doublets in tramline configurations significantly limits the possible number of doublets that produce from the same resource. To avoid negative interference, determination of the required doublet distance should be based on the doublet with the lowest production rate (Figs. 10 and 13). In that case, after the life time is reached for the doublet with the highest production rate, production could continue in the doublet with the lowest rate and negative impact on exploitation is minimised. In general larger doublet distances are required if the production rate contrast between the doublets increases. This applies to optimal doublet distance in checkboard configurations as well as minimal doublet distance in both configurations.

By using tramline and checkboard configurations in our simulations, the two most extreme interference scenarios were compared. In tramline configurations with equal well spacing, negative interference is as large as possible because both the injectors and producers reduce each other's injectivity and productivity negatively. If one of the two doublets had a larger spacing, the negative effect of one of the two wells on the other doublet would be reduced. In contrast, the most positive interference could be achieved in checkboard configurations with equal well spacing. Again, this positive interference would be smaller if one of the two doublets had a larger spacing or a different orientation. Despite these restrictions for specific scenarios, the relations in Figs. 12 and 14 can be used to describe the impact of the parameters in our study on interference. The magnitude of interference would also be larger if the number of doublets increased [11]. We only used two doublets to analyse interference. For multiple doublets in tramline configurations, minimal doublet distance will increase as less space is available for the cold water plumes. In contrast, the optimal doublet distance will shift to smaller values as thermal breakthrough is delayed longer if a doublet is surrounded by more doublets. After thermal breakthrough, however, the reduction of the production temperature could be also be increased when more doublets are used as cold water fronts from multiple doublets reach production wells.

#### 4.4. Regional development

The results of this study underline the importance of a regionally coordinated exploitation strategy. This also has been suggested to benefit ATEs as well as high enthalpy geothermal systems (e.g. [9,10,22]). A regional doublet deployment approach could aim for positive interference and avoid negative interference resulting from tramline configurations as well as production rate contrasts. These features require larger doublet distances, resulting in lower total installed capacity and lower heat recovery efficiency. In the more advantageous checkboard configuration, a lower injector-producer well spacing can be used while positive interference maintains sufficient life time. This can reduce the required doublet distance even further and increase the possible number of doublets producing from the same resource. Regional doublet deployment will mainly have an impact on life time interference. The results of this study indicate that interference in HSA exploitation is only significant in terms of life time (Fig. 9). Net energy production and NPV are only affected by less than 1% by the proximity of another doublet. In comparison, the impact of geological uncertainties on net-energy production and NPV are an order of magnitude larger (e.g., [25]). In our study NPV is determined over a 15 year period because of the Dutch feed-in tariff duration [24]. Interference could affect NPV more significantly when it is determined for a period of time that exceeds the thermal breakthrough time (e.g. Ref. [10]). In geothermal systems

where volumetric reinjection rates are lower than the production rates, interference will affect injectivity and productivity more significantly due to pressure depletion (e.g., [22]).

Finally it should be mentioned that optimisation of doublet deployment requires a regional geological model including aquifer heterogeneities and their uncertainties. Such a model requires upfront investment for cores, logs and data analysis. However, over a longer time period, the benefits can outweigh investments as negative interference is avoided and doublet placement could be optimised to meet the operator requirements.

## 5. Conclusion

On the basis of our multi parameter analysis we can conclude that:

- The fluid pressure interference in HSA exploitation has a significant impact on doublet life time as it influences cold water plume development. The impact on net energy productivity and NPV is an order of magnitude smaller.
- Optima in positive life time interference are recognized for doublets in checkboard configurations.
- Production rate contrasts between adjacent doublet systems and minimal production temperature influence the required doublet distance.
- Coordinated doublet deployment and smaller well spacing could significantly increase the possible number of doublets.

## Acknowledgements

Harmen Mijnlief (TNO Geological Survey of the Netherlands) is thanked for the discussions and support. Geothermal operators in the Netherlands are thanked for the discussions and for sharing their geological and production data. We kindly thank the consortium of share- and stakeholders of the Delft Geothermal Project (DAP) for their support. We thank the Editor and the anonymous reviewers for their constructive reviews and feedback that significantly improved the initial manuscript.

## References

- [1] Bierkens MFP, Weerts HJT. Block hydraulic conductivity of cross-bedded fluvial sediments. *Water Resour Res* 1994;30(10):2665–78.
- [2] Bisdom K, Bertotti G, Nick HM. The impact of different aperture distribution models and critical stress criteria on equivalent permeability in fractured rocks. *J Geophys Res Solid Earth* 2016;121(5):4045–63.
- [3] Boxem TAP, van Wees JD, Pluymaekers MPD, Beekman F, Batini F, Bruhn D, Calcagno P, Manzella A, Schellschmidt R. 2011. ThermoGIS world aquifer viewer - an interactive geothermal aquifer resource assessment web-tool. In: 1st EAGE Sustainable Earth Sciences (SES) conference and exhibition 2011, Valencia, Spain.
- [4] Crooijmans RA, Willems CJL, Nick HM, Bruhn DF. The influence of facies heterogeneity on the doublet performance in low-enthalpy geothermal sedimentary reservoirs. *Geothermics* 2016;64:209–19.
- [5] Daniilidis A, Doddema L, Herber R. Risk assessment of the Groningen geothermal potential: 520 from seismicity reservoir uncertainty using a discrete parameter analysis. *Geothermics* 2016;64:271–88.
- [6] Hamm V, Lopez S. 2012. Impact of fluvial sedimentary heterogeneities on heat transfer at a geothermal doublet scale. In: Stanford geothermal workshop, Jan 2012, Stanford, United States. SGP-TR-194, 18.
- [7] Hardebol NJ, Maier C, Nick H, Geiger S, Bertotti G, Boro H. Multiscale fracture network characterization and impact on flow: a case study on the Latemar carbonate platform. *J Geophys Res Solid Earth* 2015;120(12):1–26.
- [8] Jaxa-Rozen M, Kwakkel J, Bloemendaal M. The adoption and diffusion of common-pool resource-dependent technologies: the case of aquifer thermal energy storage systems. 2015.
- [9] Lopez S, Hamm H, Le Brun M, Schaper L, Boissier, Cotiche C, et al. 40 years of Dogger aquifer management in Ile-de-France, Paris Basin, France. *Geothermics* 2010;39:339–56.
- [10] Malafeh S, Sharp B. 2014. Geothermal development: challenges in a multiple access scenario. In: Proceedings 39th workshop on geothermal reservoir engineering, Stanford, California.
- [11] Mijnlief H, Van Wees JD. Rapportage ruimtelijke ordening geothermie. 2009. TNO report.
- [12] Mottaghy D, Pechig R, Vogt C. The geothermal project Den Haag: 3D numerical models for temperature prediction and aquifer simulation. *Geothermics* 2011;40:199–210.
- [13] Nick HM, Schotting R, Gutierrez-Neri M, Johannsen K. Modeling transverse dispersion and variable density flow in porous media. *Transp porous media* 2009;78(1):11–35.
- [14] Nick HM, Paluszny A, Blunt MJ, Matthai SK. Role of geomechanically grown fractures on dispersive transport in heterogeneous geological formations. *Phys Rev E* 2011;84(5). 056301.
- [15] Ogata A, Banks RB. A solution of the differential equation of longitudinal dispersion in porous media. Technical report. Washington, D.C: U.S. Geological Survey; 1961.
- [16] Pluymaekers MPD, Kramers L, van Wees JD, Kronimus A, Nelskamp S, Boxem T, et al. Aquifer characterisation of aquifers for direct heat production: methodology and screening of the potential aquifers for the Netherlands. *Neth J Geosciences* 2012;91(4):621–36.
- [17] Poulsen S, Balling N, Nielsen S. A parametric study of the thermal recharge of low enthalpy geothermal reservoirs. *Geothermics* 2015;53:464–78.
- [18] Saeid S, Al-Khoury R, Nick HM, Barends F. Experimental–numerical study of heat flow in deep low-enthalpy geothermal conditions. *Renew Energy* 2014;62:716–30.
- [19] Saeid S, Al-Khoury R, Nick HM, Hicks MA. A prototype design model for deep low-enthalpy hydrothermal systems. *Renew Energy* 2015;77:408–22.
- [20] Sommer W. Modelling and monitoring of aquifer thermal energy storage; impacts of heterogeneity, thermal interference and bioremediation. PhD thesis. Wageningen University; 2015.
- [21] TNO. NI olie- en gasportaal. 1977. [www.nlog.nl](http://www.nlog.nl).
- [22] Tureyen Oi, Sarak H, Altun G, Satman A. A modeling based analysis of unitized production: understanding sustainable management of single-phase geothermal resources with multiple lease owners. *Geothermics* 2015;55: 159–70.
- [23] Van Heekeren V, Bakema G. 2015. The Netherlands country update on geothermal energy. In: Proceedings world geothermal congress, Melbourne.
- [24] Van Wees JDAM, Kramers I, Kronimus RA, Pluymaekers MPD, Mijnlief HF, Vis GJ. ThermoGIS V1.0, Part II: methodology. 2010. TNO-Report.
- [25] Willems CJL, Goense T, Nick HM, Bruhn DF. 2016. The relation between well spacing and net present value in fluvial hot sedimentary aquifer geothermal doublets; a west Netherlands basin case study. In: 41st Workshop on geothermal aquifer engineering Stanford University 2016, Stanford, California.
- [26] Willems CJL, Nick HM, Donselaar ME, Weltje GJ, Bruhn DF. On the connectivity anisotropy in fluvial Hot Sedimentary Aquifers and its influence on geothermal doublet performance. *Geothermics* 2017a;65:222–33.
- [27] Willems CJL, Nick HM, Goense T, Bruhn DF. The impact of reduction of doublet well spacing on the Net Present Value and the life time of fluvial Hot Sedimentary Aquifer doublets. *Geothermics* 2017b;68:54–66.